



Deposited via The University of Leeds.

White Rose Research Online URL for this paper:

<https://eprints.whiterose.ac.uk/id/eprint/147470/>

Version: Accepted Version

Proceedings Paper:

Chudpooti, N, Praesomboon, S, Duangrit, N et al. (2020) An X-band Portable 3D-printed Lens Antenna with Integrated Waveguide Feed for Microwave Imaging. In: Proceedings of the 2019 Photonics & Electromagnetics Research Symposium - Spring (PIERS-Spring). 2019 Photonics & Electromagnetics Research Symposium - Spring (PIERS-Spring), 17-20 Jun 2019, Rome, Italy. IEEE, pp. 487-492. ISBN: 978-1-7281-3403-1. ISSN: 1559-9450. EISSN: 1559-9450.

<https://doi.org/10.1109/PIERS-Spring46901.2019.9017614>

Personal use of this material is permitted. Permission from IEEE must be obtained for all other uses, in any current or future media, including reprinting/republishing this material for advertising or promotional purposes, creating new collective works, for resale or redistribution to servers or lists, or reuse of any copyrighted component of this work in other works. Uploaded in accordance with the publisher's self-archiving policy.

Reuse

Items deposited in White Rose Research Online are protected by copyright, with all rights reserved unless indicated otherwise. They may be downloaded and/or printed for private study, or other acts as permitted by national copyright laws. The publisher or other rights holders may allow further reproduction and re-use of the full text version. This is indicated by the licence information on the White Rose Research Online record for the item.

Takedown

If you consider content in White Rose Research Online to be in breach of UK law, please notify us by emailing eprints@whiterose.ac.uk including the URL of the record and the reason for the withdrawal request.

An X-band Portable 3D-printed Lens Antenna with Integrated Waveguide Feed for Microwave Imaging

Nonchanutt Chudpooti¹, Sukanya Praesomboon¹, Nattapong Duangrit²,
Nutapong Somjit³, and Prayoot Akkaraekthalin²

¹Department of Industrial Physics and Medical Instrumentation
Faculty of Applied Science, King Mongkut's University of Technology North Bangkok
1518 Pracharat 1 Road, Wongsawang, Bangsue, Bangkok 10800, Thailand

²Department of Electrical and Computer Engineering, Faculty of Engineering
King Mongkut's University of Technology North Bangkok

1518 Pracharat 1 Road, Wongsawang, Bangsue, Bangkok 10800, Thailand

³School of Electronic and Electrical Engineering, University of Leeds, Leeds LS2 9JT, UK

Abstract— This paper presents a portable 3D-printed lens antenna fed by a standard rectangular waveguide at X-band for object classification. The proposed lens antenna can integrate with the standard rectangular waveguide without any additional assistant tools. A high impact polystyrene is used to design the 3D-printed hemispherical lens antenna by using the fused deposition modelling technique. This additive manufacturing gives several advantages including rapid prototyping, better cost and time effectiveness. Five lens radiuses, e.g., 20 mm, 30 mm, 40 mm, 50 mm, and 60 mm, are investigated to increase the gain of the antenna. The optimum dielectric tapered transition dimensions are simulated and obtained by using the 3D EM Simulation tool CST Studio, resulting in the reflection coefficient (S_{11}) of five lens antennas better than -10 dB across the WR-90 band. From the simulation results, the lens radiuses of 20 mm, 30 mm, 40 mm, 50 mm, and 60 mm, provide the average realized gain of 12.9 dBi, 15.2 dBi, 16.7 dBi, 17.7 dBi, and 18.6 dBi, respectively. To confirm the antenna performances of the proposed design, two lens radiuses, e.g., 20 mm and 30 mm are selected to fabricate. The gains of the lens radius of 20 mm and 30 mm are 12.1 dBi, and 14.2 dBi, respectively. The half-power beamwidth (HPBW) of lens radius of 20 mm and 30 mm are approximately 35° and 24° , respectively. The proposed dielectric lens antenna also offers other advantages, such as ease of design, low fabrication and material cost, and ease of mount and un-mount with WR-90 waveguide flange. Moreover, the narrow HPBW of lens antenna fed by standard waveguide can be applied to improve the resolution of the imaging system.

1. INTRODUCTION

3D printing technology is an exciting research area, which has received much attention in recent years. This technology allows 3D objects with optional configuration to be automatically created layer by layer in a plug and play fashion. When comparing with conventional manufacturing technique, 3D printing offers several advantages, including the capability of more flexible design, less prototyping time, cost reduction, and a faster product development cycle. The microwave, mm-wave and THz components have been fabricated using 3D printing techniques such as antennas [1, 2], waveguides [3], and sensors [4, 5]. There are several techniques for fabricating microwave, millimeter-wave and THz devices using 3D printing techniques such as fused deposition modeling (FDM), digital-light-processing (DLP) and polymer jetting (PolyJet).

An FDM [6, 7] is the first 3D printing process that uses a continuous filament of a thermoplastic material. This is fed from a spool, through a moving, heated printer extruder head. However, this technique provides the lowest printing resolution and high surface roughness, as compared with the other techniques. The DLP [8, 9] technique uses ultraviolet (UV) to create a pattern by selectively curing a resin-based photopolymer. The resolution of this technique depends on UV light spot size. Commonly, this technique can produce a printing resolution in each layer of approximately 25–100 μm . The PolyJet technique is similar to inkjet printing, as its uses a nozzle head to droplet liquid polymer onto a building platform and the liquid polymers are cured and 3D patterned by UV light. This technique offers the finest printing resolution and printing accuracy. For creating microwave, millimeter-wave and THz devices, the technique of 3D printing, which is used to create the prototype, is considered because the printing resolution may affect to performance of printed device in each application.

In this paper, a low-cost 3D printed dielectric lens antenna using the 3D FDM technique is proposed, operating at X-band from 8.2 GHz–12.4 GHz, and directly fed by a standard WR-90 rectangular waveguide. The proposed dielectric lens antenna is designed by using basic hemispherical structure. High-impact polystyrene (HIPS), a widely commercial photopolymer material that has a free-space measurement property, is the investigated material and is selected to design the hemispherical lens antenna. The taper transition is implemented to reduce impedance mismatch between waveguide and lens antenna, resulting in a decreased reflection coefficient, S_{11} . Five radiuses of the lens antennas, e.g., 20 mm, 30 mm, 40 mm, 50 mm and 60 mm, are investigated to monitor antenna performances, e.g., realized gain, and the half-power beamwidth (HPBW). To prove the concept of the proposed lens antenna design, two lens radiuses are chosen and fabricated. The maximum gain of the two lens radiuses of 20 mm and 30 mm are 14.1 dBi, and 15.5 dBi, respectively. The operating bandwidth of both lens antennas is 40.8% (8.2 GHz–12.4 GHz). The HPBW of two lens radiuses, e.g., 20 mm and 30 mm, are approximately 35° and 24° , respectively.

2. 3D-PRINTED LENS ANTENNA DESIGNS, FABRICATIONS AND INTEGRATIONS

2.1. 3D-Printed Lens Antenna Designs

The proposed hemispherical lens antenna, which fed by WR-90 rectangular waveguide, is designed based on 3D FDM printing technique. The HIPS material is used to design the 3D-printed lens antenna owing to its low cost and standard commercial material. The relative permittivity and loss tangent of the HIPS material, which were investigated in [10], are 2.45 and 5.75×10^{-4} , respectively. Figure 1 shows the 3D perspective view of the 8.2–12.4 GHz lens antenna.

The geometry of the proposed lens antenna composed of two sections. The first section is part for wave propagation of the antenna, which consists of the lens radius, R , and extension length of the lens antenna, L . In this work, the lens radius and extension length of the hemispherical lens antenna are fixed to ratio between the extension length and lens radius (L/R) of 1, which were investigated in [11]. The second section of the proposed lens is taper transition, which composed of chamfer angle, θ , taper height, T_H , taper width, T_W , and taper length, T_L . The taper transition is created to reduce impedance mismatch between the waveguide and lens antenna. The taper height, T_H , and taper width, T_W , are 10.16 mm and 22.96 mm, respectively, which similar to the aperture size of the WR-90 rectangular waveguide. The 3D EM Simulation tool CST Studio was used to optimize the dielectric tapered transition dimensions, e.g., chamfer angle, θ , and taper length, T_L , resulting in the reflection coefficient, S_{11} , of lens antennas better than -10 dB across the operating band from 8.2–12.4 GHz. To study the performance of the lens antenna, five lens radiuses, e.g., $R = 20$ mm, $R = 30$ mm, $R = 40$, $R = 50$ mm, and $R = 60$ mm, are investigated. The simulated realized gain of without lens and with five lens radiuses at the radiation direction of 0° were plotted in Figure 2(a). The lens radius of 20 mm, 30 mm, 40 mm, 50 mm, and 60 mm provide the average realized gain of 12.9 dBi, 15.2 dBi, 16.7 dBi, 17.7 dBi, and 18.6 dBi, respectively. Figure 2(b) shows the simulated radiation pattern at center operating frequency band (10.3 GHz) without and with five lens radiuses. The calculated HPBW of five samples, e.g., $R = 20$ mm, $R = 30$ mm, $R = 40$, $R = 50$ mm, and $R = 60$ mm, are approximately 35° , 24° , 19° , 16° , and 7° , respectively. From simulation results, the gain and the HPBW of the lens antenna can be selected from radius of lens antenna. To prove the simulation result, two lens radiuses, e.g., 20 mm and 30 mm, are chosen and fabricated. The necessary parameters of two lens antennas are listed in Table 1.

Table 1. The 3D-printed hemispherical lens antenna geometry of 20 mm lens radius and 30 mm lens radius.

Parameters	Descriptions	Optimum value of lens antenna of $R = 20$ mm	Optimum value of lens antenna of $R = 30$ mm
R	Radius of lens antenna	20 mm	30 mm
L	Extension length of lens antenna	20 mm	30 mm
θ	Chamfer angle of tapered transition	35 degree	40 degree
T_L	Taper length	10.16 mm	10.16 mm

2.2. 3D-Printed Lens Antenna Fabrications and Integration

The proposed lens antenna was fabricated by using the Zortrax M200 [12] featuring FDM manufacturing technique. The (HIPS), which the Zortrax recommends using for parts and models requiring

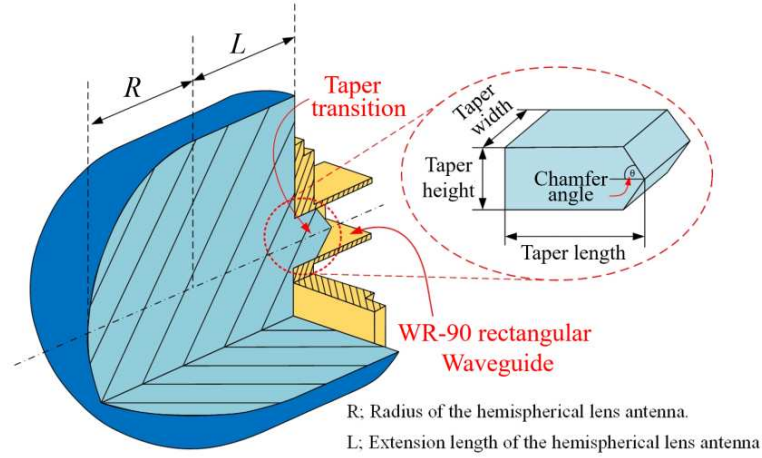


Figure 1. A 3D geometry of hemispherical lens antenna consists of a standard WR-90 rectangular waveguide and 3D-printed lens antenna. Two important parameters, e.g., the lens radius, R , and the extension length of hemispherical lens antenna, L , are used to design the proposed lens antenna.

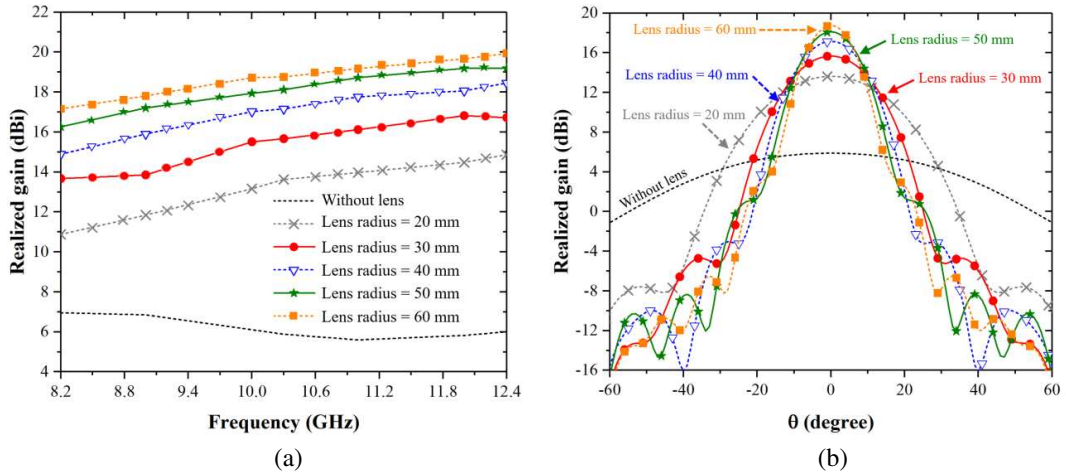


Figure 2. (a) The simulated realized gain of without lens and with five lens radiuses, e.g., 20 mm, 30 mm, 40 mm, 50 mm and 60 mm, at the radiation direction of 0° . (b) The simulated radiation pattern of without lens and with five lens radiuses, e.g., 20 mm, 30 mm, 40 mm, 50 mm and 60 mm, at the radiation direction of 0° .

a smooth surface, was chosen as the material for fabricating the proposed lens antenna. The completed 3D models of the proposed lens antennas were exported from the 3D EM Simulation tool CST Studio using the STL file format. The STL code from 3D EM Simulation tool was converted to the Zortrax machine language (G-code) by using the Z-SUIT Zortrax dedicated slicing software with the layer thickness set to $90 \mu\text{m}$, nozzle diameter 0.4 mm , and 100% infill density (solid object). The total printing time of two lens radiuses, e.g., $R = 20 \text{ mm}$ and $R = 30 \text{ mm}$ was approximately 15 hours and 26 hours, respectively. Figures 3(a) and (b) show the fabricated lens antenna before and after mounting with WR-90 waveguide to coax adapter, respectively.

3. MEASUREMENT RESULTS

A Rohde & Schwarz ZVB-20 vector network analyzer (VNA) was used with Through-Open-Short-Match (TOSM) calibration to measure the reflection coefficient and radiation pattern of the two fabricated lens antennas. The simulated and measured reflection coefficient, S_{11} , and realized gain at 0° of two lens antennas from 8.2–12.4 GHz are plotted in Figure 4. From the measurement results, both lens antennas archive the reflection coefficient below 11 dB. The average gain of the lens radius $R = 20 \text{ mm}$ and $R = 30 \text{ mm}$ for the whole WR-90 band are 12.1 dBi, and 14.2 dBi, respectively. To measure the radiation pattern of the proposed lens antenna, a WR-90 horn antenna with average gain of 15 dBi was used as the reference antenna. The DAMs Heavy-Duty Antenna Model-5100,

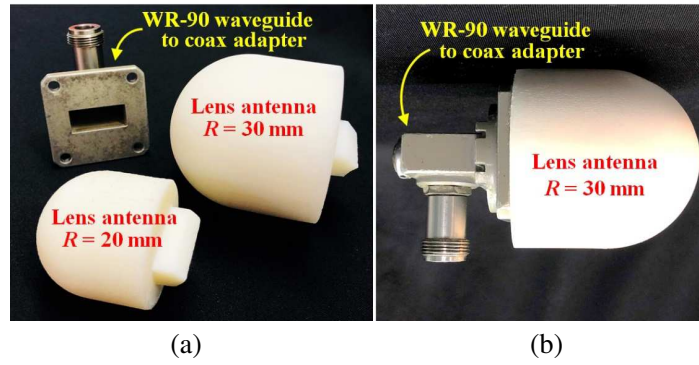


Figure 3. (a) Two fabricated lens antenna, e.g., $R = 20$ mm and $R = 30$ mm, with WR-90 waveguide to coax adapter before integration, (b) the sample of lens antenna $R = 30$ mm was mounted to WR-90 waveguide to coax adapter.

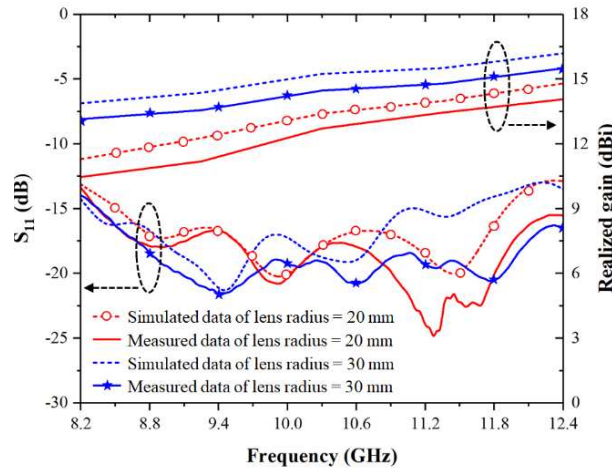


Figure 4. The simulated and measured of reflection coefficient, S_{11} and realized gain at 0° direction of the two lens antennas.

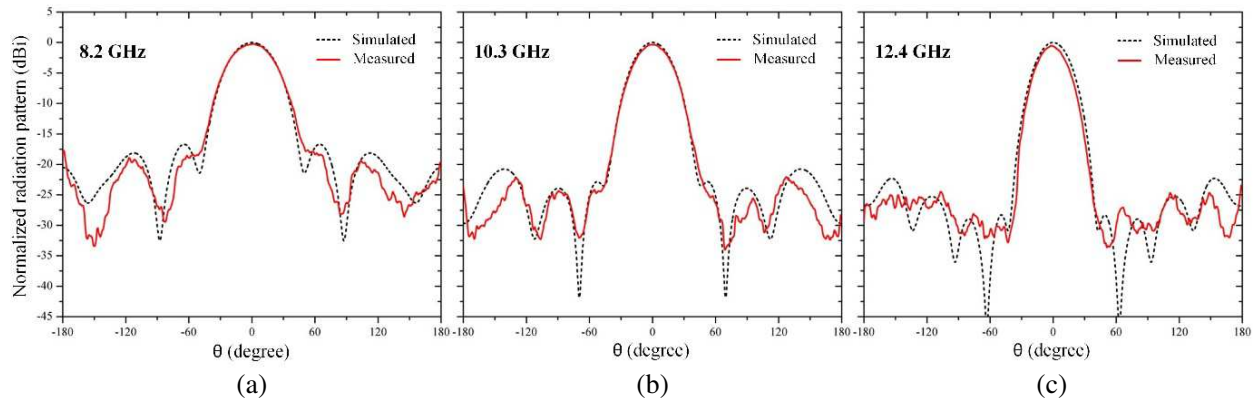


Figure 5. The simulated and measured radiation pattern of lens antenna radius of 20 mm for (a) 8.2 GHz, (b) 10.3 GHz and (c) 12.4 GHz.

a turntable for rotating the antenna under test (AUT), was connected with the Rohde & Schwarz ZVB-20 VNA. The Antenna Measurement Studio Software [13] of Diamond Studio was used to control and to collect the transmission coefficient, S_{21} , between the reference antenna and the AUT. The distance between the reference antenna and the AUT was set to 1 m, which is beyond the calculated far-field distance at the highest frequency of the AUT. The AUT was automatically rotated from 0° to 360° with a step of 1° by using DAMs Heavy-Duty Antenna Model-5100. The radiation pattern of two lens antenna, e.g., $R = 20$ mm and $R = 30$ mm, at three frequencies,

e.g., 8.2 GHz (low-band), 10.3 GHz (middle-band), and 12.4 GHz (high-band), were measured and plotted in Figure 5, and Figure 6, respectively. The measured results of both antennas show good agreement when compared with simulation results. The measured HPBW of two lens antennas, e.g., $R = 20$ mm and $R = 30$ mm, are approximately 35° and 24° , respectively.

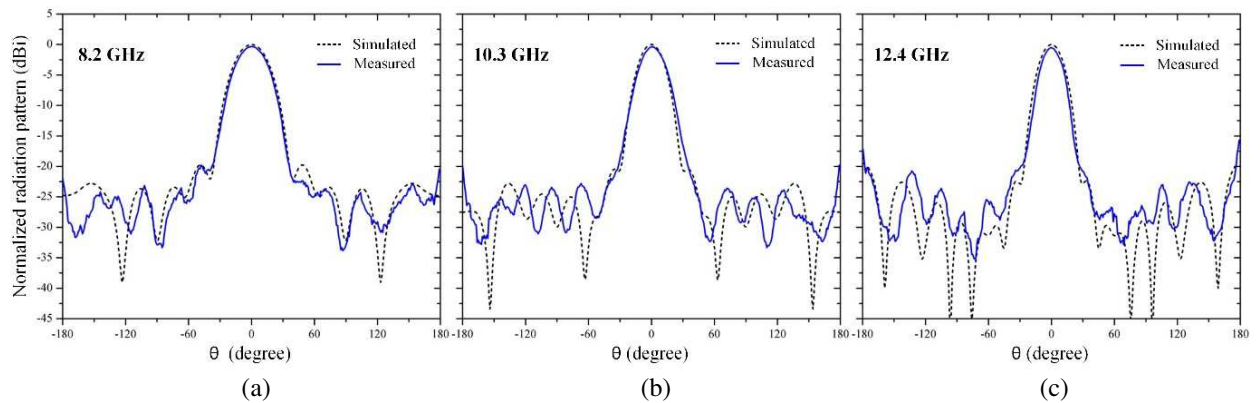


Figure 6. The simulated and measured radiation pattern of lens antenna radius of 30 mm for (a) 8.2 GHz, (b) 10.3 GHz and (c) 12.4 GHz.

4. CONCLUSIONS

A portable 3D-printed hemispherical lens antenna, operating over the X-band has been reported. The lens antenna was designed and fabricated by using an FDM printing technology with HIPS, which is a commercial polymer material. Two proposed lens antennas, e.g., 20 mm and 30 mm, provide maximum gain at 0 degree of 14.1 dBi, and 15.5 dBi, respectively. The fractional bandwidth of antenna is 40.8% (8.2 GHz–12.4 GHz). The lens antenna in this paper offers various key advantages over any state-of-the-art, e.g., low-profile, ease of design and integration with WR-90 waveguide, low-cost and low fabrication process. Moreover, the narrow HPBW of the proposed lens antenna can be applied to improve the resolution in imaging applications.

ACKNOWLEDGMENT

This work has been supported in part by the Thailand Research Fund through the TRF Senior Research Scholar Program under Grant RTA 6080008, and in part by the Royal Golden Jubilee Ph.D. Program under Grant PHD/0056/2558.

REFERENCES

1. Kwon, O. H., et al., "3D-printed super-wideband spidron fractal cube antenna with laminated copper," *Appl. Sci.*, Vol. 7, 797, 2017.
2. Vorobyov, A., J. R. Farserotu, and J.-D. Decotignie, "3D printed antenna for mm-wave sensing application," *2017 11th Int. Symp. Med. Inf. and Commun. Technol. (ISMICT)*, 23–26, Lisbon, Apr. 2017.
3. Kyovtorov, V., et al., "New antenna design approach-3D polymer printing and metallization. experimental test at 14–18 GHz," *AEU-Int. J. Electron. Commun.*, Vol. 73, 119–128, Mar. 2017.
4. Kimionis, J., et al., "3D-printed origami packaging with inkjet-printed antennas for RF harvesting sensor," *IEEE Trans. Microw. Theory Tech.*, Vol. 63, No. 12, Dec. 2015.
5. Gross, B. C., et al., "Evaluation of 3D printing and its potential impact on biotechnology and the chemical science," *American Chemical Soc.*, Vol. 86, 3240–3253, 2014.
6. Varosis, A. B., "Introduction to FDM 3D printing," [Online], Available at <https://www.3dhubs.com/knowledge-base/introduction-fdm-3d-printing/#author>, 2019.
7. Alsofí, M. S. and A. E. Elsayed, "How surface roughness performance of printed parts manufactured by desktop FDM 3D printer with PLA+ is influenced by measuring direction," *American J. Mechanical Eng.*, Vol. 5, No. 5, 211–222, 2017.
8. Gregurić, L., "What is a DLP 3D printer? — simply explained," [Online], Available at <https://all3dp.com/2/what-is-a-dlp-3d-printer-3d-printing-simply-explained/>, Sep. 2018.

9. Xin, H. and M. Liang, "3D printed microwave and THz device using polymer jetting techniques," *Proc. IEEE.*, Vol. 105, No. 4, 737–755, 2017.
10. Uskov, G. K., et al., "Investigation of 3D printed dielectric structure for microwave lens prototyping," *2017 XI International Conf. Antenna Theory and Techniques (ICATT)*, 294–296, Kiev, 2017.
11. Chudpooti, N., et al., "220–320 GHz hemispherical lens antennas using digital light processed photopolymers," *IEEE Access*, Vol. 7, 12283–12290, 2019.
12. Zortrax, "Specification and operational characteristics of Zortrax M series 3D printer," [Online], Available at <https://support.zortrax.com/m-series-specification/>, 2019.
13. Diamond Engineering, "Antenna measurement software," [Online], Available at http://www.diamondeng.net/PDF/software_specs.pdf, 2018.